High-resolution epi-illumination raster-scan optoacoustic mesoscopy for imaging of model organisms and microvessels

Murad Omar,[1] Dominik Soliman[1], Jérôme Gateau[2], and Vasilis Ntziachristos[1,*]

[1]*Chair for Biological Imaging, Technische Universität München and Helmholtz Zentrum München, German Research Center for Environment and Health, Institute for Biological and Medical Imaging, Ingolstädter Landstraße 1, 85764 Neuherberg, Germany*
[2]*ESPCI ParisTech, PSL Research University, CNRS, INSERM, Institut Langevin, 1 rue Jussieu, F-75005, Paris, France*

Short Abstract – We have developed an epi-illumination raster-scan optoacoustic mesoscopy, the system achieved a resolution of 18 µm laterally, and 4 µm axially. To showcase the system we imaged a zebrafish ex-vivo, and an excised mouse ear.

Abstract – We have developed an epi-illumination raster-scan optoacoustic mesoscopy system (RSOM), the new system is capable of imaging model organisms, and vasculature. The newly developed system is based on a custom designed; spherically focused detector with a Characterization of the system shows an isotropic lateral resolution of 18 μm, and an axial resolution of 4 μm. The scan times are on the order of 8 minutes for a field of view of 10×10 mm^2. The achieved resolution is slightly degraded up to a depth of 5 mm. After characterizing the system we showcase it's performance on a zebrafish ex vivo, and an excised mouse ear. Additionally, to improve the visibility of small structures we have reconstructed the high frequencies, and the low frequencies separately, and at the end overplayed the two reconstructions using different colors, this way the high frequencies are not masked by the low frequencies which have a higher signal to noise ratio.

Keywords – mesoscopy, microcirculation, optoacoustic, photoacoustic, skin, frequency analysis

1. INTRODUCTION

Imaging at different scales is fundamental for the proper understanding of biological processes. Microscopic techniques, both fluorescence and optoacoustic both depend on the use of focused beams of light[1-4], this fundamentally limits the imaging depth of those techniques to several hundreds of microns. Tomographic techniques on the other hand, such as optoacoustic tomography, fluorescence molecular tomography, and similar can image deeper than microscopic techniques, but this comes at the expense of the resolution. Thus, although a depth of tens of millimeters could be achieved, this happens at a resolution of > 100 µm. This again limits this technique to large samples, such as full mice[5-7]. Thus imaging becomes suitable only for samples which have a diameter > 5 mm. This essentially creates an imaging gap, which we call the mesoscopic gap.

Several systems have been introduced to close this gap. Yet most of these solutions were based on lower frequencies[8-11]. In this work we investigate the effect, and the benefit of using a high-frequency ultrasonic detector, on the overall resolution, and the achievable penetration depth.

Previously we have introduced raster-scan optoacoustic mesoscopy (RSOM), employing a 100 MHz spherically focused ultrasound detector, as a method to fill the mesosopic gap[12]. Although the first generation of RSOM managed to image, genetically modified drosophila pupae, and zebrafish[12]. It's main limitation; from a wider deployment was the illumination. Because of the physical size of the detector, see figure 1a, trans-illumination was used, thus effectively; only thin samples could be imaged. For a wider deployment of the system, for imaging skin,

Opto-Acoustic Methods and Applications in Biophotonics II, edited by Vasilis Ntziachristos, Roger Zemp,
Proc. of SPIE Vol. 9539, 95390U · © 2015 SPIE · CCC code: 1605-7422/15/$18 · doi: 10.1117/12.2183624

and cancer development, for example, epi-illumination needs to be used. For this we used a custom designed ultrasonic detector, with a conically shaped acoustic lens. This new design enabled coupling the light from the same side as the detector, at an angle of 45°-60°.

2. METHODS AND MATERIALS

In the new, reflection mode RSOM we used a high frequency ultrasonic detector, with a bandwidth of 20-180 MHz. The detector had a focus of 1.65 mm, and an *f-number* of ~1.1, which results in a good resolution in the focus, and a good angular coverage outside of the focus. The choice of the detector was based on the need for high sensitivity, thus large aperture, and at the same time good resolution, thus the acoustic lens.

The excitation was performed with a diode pumped solid state laser (DPSS) (Wedge-HB532, BrightSolutions), working at 532 nm, the laser light is coupled to the sample through a fiber-bundle with 3 outputs, which optimizes the illumination of the sample in and around the focus of the acoustic detector. The laser is capable of pulsing at a maximum repetition rate of 2 kHz. This high repetition rate is a necessity for fast scanning of the sample. The detected optoacoustic signals are amplified using a low noise, high gain amplifier (AU-1291, MITEQ Inc.). After amplification the signals are digitized using a 12-bit, card operating at 1 GS/s (Gage-applied).

The scan is performed in a hybrid continuous-discrete mode, where one of the axes is scanned continuously, while the other axis is scanned discretely. This scan enables faster scanning of sample. The step size is 10 µm in both the *x* and *y* directions. Thus a scan of 10×10 mm^2 takes around ~8 minutes[13].

For reconstruction, beam forming with a dynamic aperture was used[12, 13]. The dynamic aperture accounts for the angular coverage of the detector. Using this method enabled us to retain the focal capabilities even outside of the acoustic focus. For best results the voxel size of the reconstruction is $10 \times 10 \times 3$ µm^3. As low frequencies have a higher amplitude, and higher *SNR* in comparison to high-frequencies, thus on the final image the small structures corresponding to high-frequencies are masked, to overcome this we have used a dual band reconstruction, where we reconstruct the low frequencies separately from the high frequencies, and we then overlay them on the final image using different colors.

To characterize the system we used 3 µm polysterene black spheres, and 10 µm sutures. Figure 2.a shows the reconstruction of the microspheres, where the maximum intensity projection of the three-dimensional reconstruction has been taken.

Finally, for showcasing the capabilities of the system we have used an excised mouse ear, and a zebrafish *ex vivo*.

3. RESULTS

Characterization using microspheres revealed an isotropic resolution of 18 µm laterally, and 4 µm axially, see figure 2.a. On the other hand moving a suture through the different depths shows that the resolution minimally degrades with depth, up to a depth of 5 mm, see figure 2.b[13].

Imaging results are shown in figure 3, where figure 3.a shows an image of the zebrafish. Red shows the total bandwidth, while cyan shows the high-frequencies, i.e. 100-180 MHz. In a similar manner the data of a mouse ear are reconstructed, and again in red the total bandwidth is shown, while in cyan the high-frequencies, i.e. 100-180 MHz are shown.

4. DISCUSSION AND CONCLUSION

We have introduced here a reflection mode RSOM system. A custom designed, ultrawideband acoustic detector enabled this technical progress. To capitalize on the ultrawideband capability, we used a dual bandwidth reconstruction, where we reconstruct the low frequencies separately from the high frequencies. This enabled better discrimination between small and large structures, as well as improved the *SNR* and the contrast of the high frequencies.

The reason why such a reconstruction improved the resolution, and the contrast for low frequencies lies in the basic optoacoustic effect. Where generally if the heat confinement, and the stress confinement conditions are met, then the amplitude of the optoacoustic signal is proportional to the diameter of the object excited. Thus high-frequencies, corresponding to small structures have smaller amplitude, compared to low-frequencies corresponding to large objects. Additionally, high-frequencies exhibit higher attenuation while propagating through the tissue, compared with low frequencies, and were the attenuation is proportional to the frequency in tissue[14]. Thus all in all, the high-frequencies will have a lower *SNR* when compared to low-frequencies. This effect results in masking of the small structures by larger ones, thus the resolution generally degrades, and the small objects are not visible on the image. By using a dual-bandwidth reconstruction, this problem could be mitigated.

The technological advance introduced in this proceeding should enable not only imaging of small model organisms, but also the imaging of thick tissue such as skin, and tumor development in mice[15-17].

Future developments can include combining the method with other modalities, such as optical microscopy, optoacoustic microscopy[2, 18], or ultrasound, both active and passive[19-21], additionally improving the reconstruction can result in better resolution, and *SNR*[22].

Finally, the use of point detectors based on silicon photonics[23, 24], or new illumination techniques, such as speckle illumination can improve both the resolution, and the visibility of tilted structures[25].

5. Acknowledgements

We would like to thank Dr. Hernan Lopez-Schier for providing the samples for us. VN would like to acknowledge financial support from the ERC advanced grant “Next generation in-vivo imaging platform for post-genome biology and medicine MSOT” (233161), the DFG Reinhart Koselleck project “High resolution near-field thermoacoustic sensing and imaging” (NT 3/9-1), and the DFG as part of the CRC 1123 (AX).

6. References

[1] J. Yao and L. V. Wang, "Photoacoustic microscopy," *Laser & Photonics Reviews,* vol. 7, pp. 758-778, 2013.

[2] G.J. Tserevelakis, D. Soliman, M. Omar, and V. Ntziachristos, "Hybrid Multi-photon and Optoacoustic Microscope," *Optics Letters,* vol. 39, 2014.

[3] G. J. Tserevelakis, E. V. Megalou, G. Filippidis, B. Petanidou, C. Fotakis, and N. Tavernarakis, "Label-Free Imaging of Lipid Depositions in C. elegans Using Third-Harmonic Generation Microscopy," *PloS one,* vol. 9, p. e84431, 2014.

[4] V. Ntziachristos, "Going deeper than microscopy: the optical imaging frontier in biology," *Nature Methods,* vol. 7, pp. 603-614, 2010.

[5] S. Tzoumas, N. Deliolanis, S. Morscher, and V. Ntziachristos, "Unmixing molecular agents from absorbing tissue in multispectral optoacoustic tomography," *Medical Imaging, IEEE Transactions on,* vol. 33, pp. 48-60, 2014.

[6] V. Ntziachristos and D. Razansky, "Molecular imaging by means of Multispectral optoacoustic tomography (MSOT)," *Chemical Reviews,* vol. 110, pp. 2783-2794, 2010.

[7] S. Tzoumas, A. Zaremba, U. Klemm, A. Nunes, K. Schaefer, and V. Ntziachristos, "Immune cell imaging using multi-spectral optoacoustic tomography," *Opt Lett,* vol. 39, pp. 3523-6, Jun 15 2014.

[8] J. Laufer, P. Johnson, E. Zhang, B. Treeby, B. Cox, B. Pedley*, et al.*, "In vivo preclinical photoacoustic imaging of tumor vasculature development and therapy," *Journal of biomedical optics,* vol. 17, pp. 0560161-0560168, 2012.

[9] J. Gateau, A. Chekkoury, and V. Ntziachristos, "High-resolution optoacoustic mesoscopy with a 24 MHz multidetector translate-rotate scanner," *Journal of Biomedical Optics,* vol. 18, p. 106005, 2013.

[10] J. Gateau, M. Gesnik, J.-M. Chassot, and E. Bossy, "Single-side access, isotropic resolution, and multispectral three-dimensional photoacoustic imaging with rotate-translate scanning of ultrasonic detector array," *Journal of Biomedical Optics,* vol. 20, pp. 056004-056004, 2015.

[11] J. Gateau, A. Chekkoury, and V. Ntziachristos, "Ultra-wideband three-dimensional optoacoustic tomography," *Opt Lett,* vol. 38, pp. 4671-4, Nov 15 2013.
[12] M. Omar, J. Gateau, and V. Ntziachristos, "Raster-scan optoacoustic mesoscopy in the 25-125 MHz range," *Opt Lett,* vol. 38, pp. 2472-4, Jul 15 2013.
[13] M. Omar, D. Soliman, J. Gateau, and V. Ntziachristos, "Ultrawideband reflection-mode optoacoustic mesoscopy," *Optics Letters,* vol. 39, pp. 3911-3914, 2014.
[14] X. L. Dean-Ben, D. Razansky, and V. Ntziachristos, "The effects of acoustic attenuation in optoacoustic signals," *Phys Med Biol,* vol. 56, pp. 6129-48, Sep 21 2011.
[15] M. Omar, M. Schwarz, D. Soliman, P. Symvoulidis, and V. Ntziachristos, "Pushing the Optical Imaging Limits of Cancer with Multi-Frequency-Band Raster-Scan Optoacoustic Mesoscopy (RSOM)," *Neoplasia,* vol. 17, pp. 208-214, 2015.
[16] J. Aguirre;, M. Schwarz;, D. Soliman;, A. Buehler;, M. Omar;, and V. Ntziachristos, "Broadband mesoscopic optoacoustic tomography reveals skin layers," *Optics Letters,* vol. 39, pp. 6297-9300, 2014.
[17] M. Schwarz, M. Omar, A. Buehler, J. Aguirre, and V. Ntziachristos, "Implications of ultrasound frequency in optoacoustic mesoscopy of the skin," *IEEE transactions on medical imaging,* vol. 34, pp. 672-677, 2015.
[18] M. Kneipp, J. Turner, H. Estrada, J. Rebling, S. Shoham, and D. Razansky, "Effects of the murine skull in optoacoustic brain microscopy," *Journal of biophotonics,* vol. 9999, 2015.
[19] H. Estrada, E. Sobol, O. Baum, and D. Razansky, "Hybrid optoacoustic and ultrasound biomicroscopy monitors' laser-induced tissue modifications and magnetite nanoparticle impregnation," *Laser Physics Letters,* vol. 11, p. 125601, 2014.
[20] P. Subochev, A. Katichev, A. Morozov, A. Orlova, V. Kamensky, and I. Turchin, "Simultaneous photoacoustic and optically mediated ultrasound microscopy: phantom study," *Optics letters,* vol. 37, pp. 4606-4608, 2012.
[21] P. Subochev, A. Orlova, M. Shirmanova, A. Postnikova, and I. Turchin, "Simultaneous photoacoustic and optically mediated ultrasound microscopy: an in vivo study," *Biomedical optics express,* vol. 6, pp. 631-638, 2015.
[22] P. Mohajerani, S. Tzoumas, A. Rosenthal, and V. Ntziachristos, "Optical and Optoacoustic Model-Based Tomography: Theory and current challenges for deep tissue imaging of optical contrast," *Signal Processing Magazine, IEEE,* vol. 32, pp. 88-100, 2015.
[23] A. Rosenthal, S. Kellnberger, D. Bozhko, A. Chekkoury, M. Omar, D. Razansky*, et al.*, "Sensitive interferometric detection of ultrasound for minimally invasive clinical imaging applications," *Laser & Photonics Reviews,* vol. 8, pp. 450-457, 2014.
[24] A. Rosenthal, M. Omar, H. Estrada, S. Kellnberger, D. Razansky, and V. Ntziachristos, "Embedded ultrasound sensor in a silicon-on-insulator photonic platform," *Applied Physics Letters,* vol. 104, p. 021116, 2014.
[25] J. Gateau, T. Chaigne, O. Katz, S. Gigan, and E. Bossy, "Improving visibility in photoacoustic imaging using dynamic speckle illumination," *Optics Letters,* vol. 38, pp. 5188-5191, 2013.

7. Figures

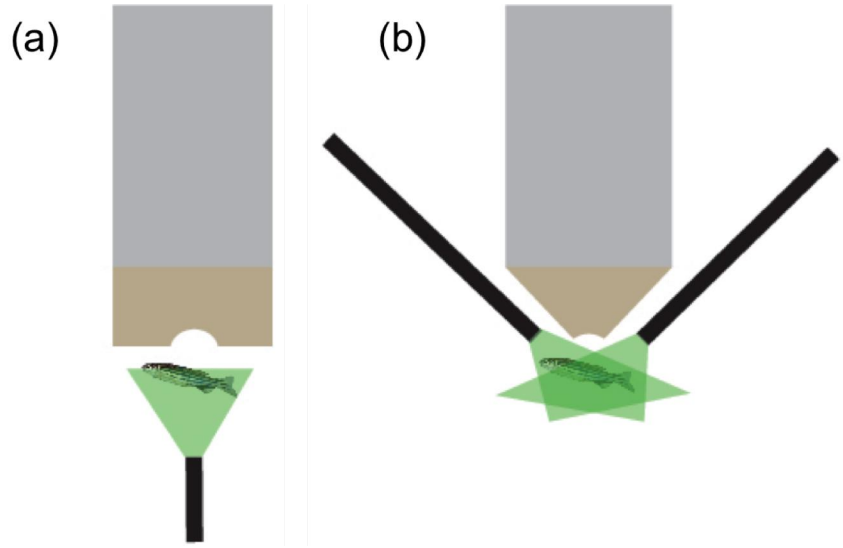

Figure 1: (a) First generation of the raster scan optoacoustic mesoscopy system, with trans-illumination. (b) Second generation of the raster-scan optoacoustic mesoscopy system, with reflection mode operation.

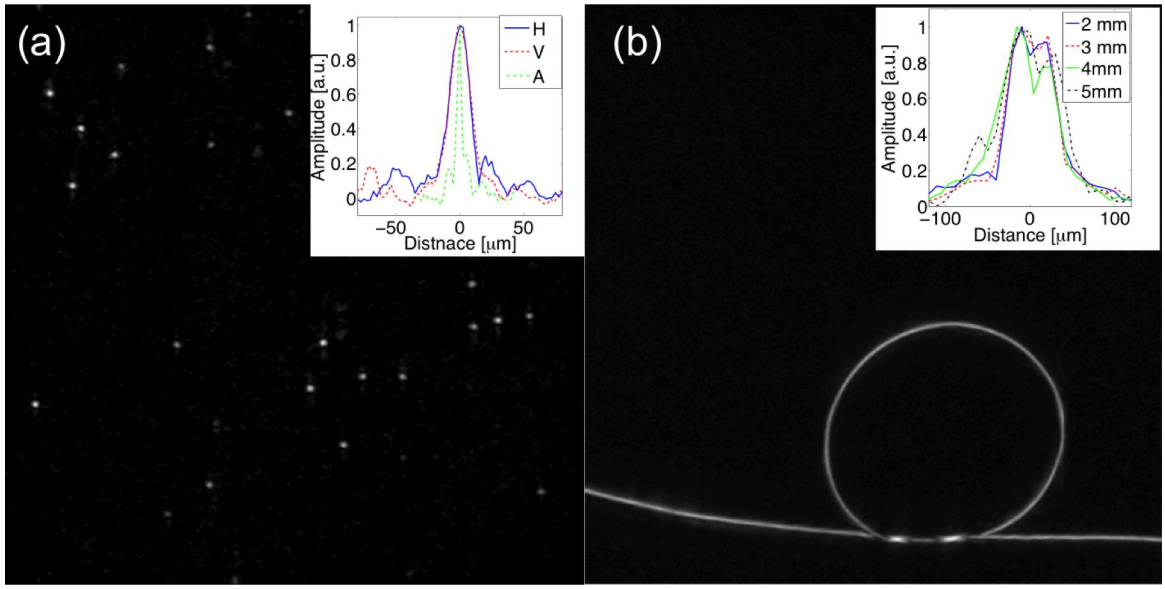

Figure 2: (a) reconstruction of the 3 μm microspheres, the inset shows the vertical (V), horizontal (H), and axial (A) profiles of one of the microspheres. (b) an image of a suture (maximum intensity projection), the inset shows a profile through the knot, and it shows that throughout a depth of 5 mm, the resolution minimally degrades.

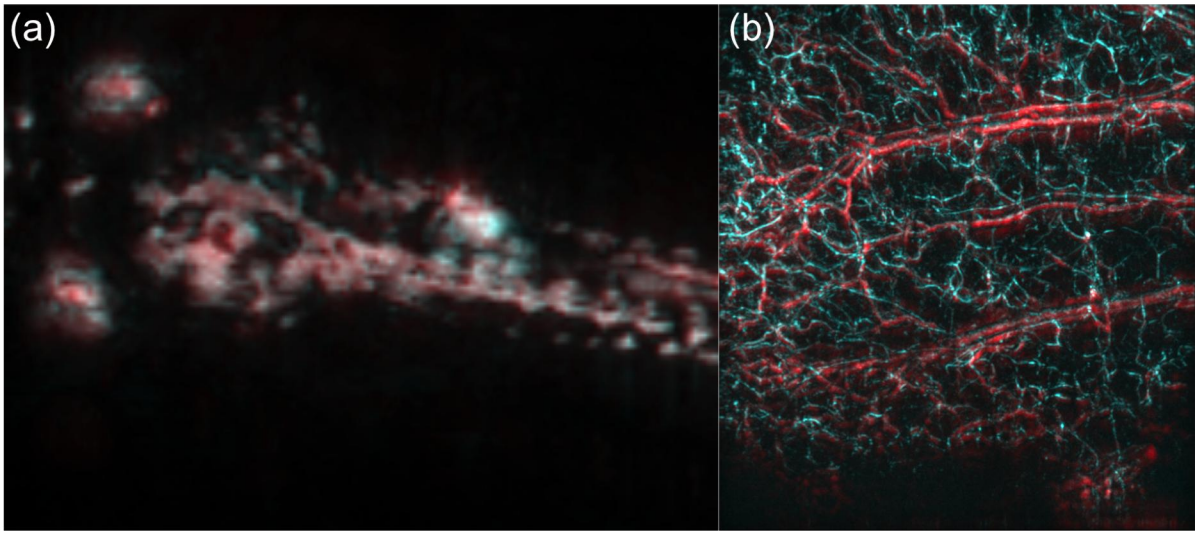

Figure 3: (a) Image of zebrafish in RSOM, the image shows the eyes, the lateral line, the intestines, and the pigments, (b) image of a mouse ear in RSOM, the image nicely combines small structures with large ones.
In both the images cyan represents high-frequencies: 100-180 MHz, and red the whole bandwidth: 20-180 MHz.